UNIVERSITÀ DEGLI STUDI DI BERGAMO
DIPARTIMENTO DI INGEGNERIA DELL'INFORMAZIONE
E METODI MATEMATICI°

QUADERNI DEL DIPARTIMENTO

Department of Information Technology and Mathematical Methods

Working Paper

Series "*Information Technology*"

n. 10/IT – 2007

Vibration control in a washing machine by using magnetorheological dampers

by

Fabio Previdi and Cristiano Spelta

° Viale Marconi. 5, I – 24044 Dalmine (BG), ITALY, Tel. +39-035-2052339; Fax. +39-035-562779

[§] L'accesso alle *Series* è approvato dal Comitato di Redazione. I *Working Papers* della Collana dei Quaderni del Dipartimento di Ingegneria dell'Informazione e Metodi Matematici costituiscono un servizio atto a fornire la tempestiva divulgazione dei risultati dell'attività di ricerca, siano essi in forma provvisoria o definitiva.

VIBRATION CONTROL IN A WASHING MACHINE BY USING MAGNETORHEOLOGICAL DAMPERS

Fabio Previdi and Cristiano Spelta

Università degli Studi di Bergamo,Facoltà di Ingegneria, 24044 Dalmine (BG), ITALY

Abstract - The aim of this work is the analysis and design of a control system for vibration and noise reduction in a washing machine. The control system is implemented via a semi-active magnetorheological (MR) damper located on the suspension that links the drum of the machine to the cabinet. The entire design procedure is outlined: first, the semi-active actuator is described and an experimental protocol is proposed and tested on an instrumented machine; two adaptive control strategies then are proposed, designed and tested. The reported results show the effectiveness of the proposed control system.

Keyterms - Semi-active suspensions; magnetorheological damper; adaptive control; non-linear system; washing machine.

1. INTRODUCTION AND PROBLEM STATEMENT

Among the many different types of electronically-controlled suspension systems (see e.g. [4, 9-12, 19-20, 37-38]), semi-active suspensions have recently received a lot of attention since they provide the best compromise between cost (energy-consumption and actuators/sensors hardware) and performance. The concept of semi-active suspensions can be applied over a wide range of application domains: road-vehicle suspensions, cabin suspensions in trucks or tractors, seat suspensions, suspensions in trains, suspensions of appliances (e.g. washing machines), architectural suspensions (buildings, bridges, etc.), bio-mechanical structures (e.g. artificial legs) etc. ([1, 7, 14, 22]).

This work focuses on the suspension of a washing machine, namely the suspension which links the drum to the machine cabinet. In this kind of appliance the aim of the suspension is to damp the drum movements and to reduce the vibrations transmitted to the chassis, which are strictly related to the perceived acoustic noise.

The research idea investigated in this work is to replace the passive dampers with devices characterized by an electronically-controlled damping ratio, and to control them according to feedback control strategies. The control objective is to reduce the vibrations measured on the cabinet panels.

The vibrations in washing machine are mainly due to the unbalanced weight of the drum. This causes movements of the suspended mass which are transmitted to the body cabinet through the suspension system.

The control techniques for vibration reduction in washing machines can be divided into two main families: techniques based on the control of the tub balance (see e.g. [27]) and techniques based on the control of the suspension system (see e.g. [7]). This work focuses on the latter class of techniques.

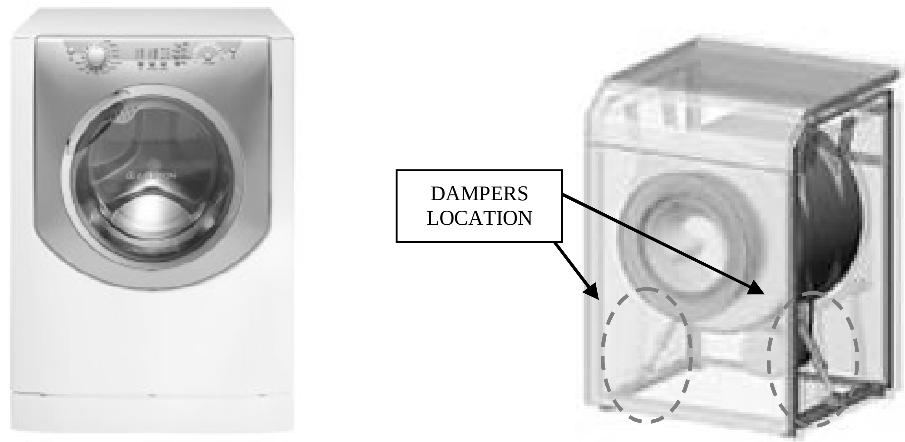

Fig.1. Left: a picture of the washing machine object of this work: the *Ariston Aqualtis* manufactured by *Indesit Company*. Right: damper location in the washing machine.

The problem of semi-active control in appliances such as washing machines is still in its very infancy; it has been recently treated and discussed only in [7], where the focus is mainly of the tub dynamics at low spin, around the main drum resonance frequency. This work instead mainly focuses on the vibrations induced at high spin velocity.

The main contributions of this work are the following:

- the characterization of the washing machine with passive standard dampers and with magnetorheological (MR) devices, and an accurate analysis of the dynamical behavior in case of different mounting solutions;
- the design, implementation and testing of two different adaptive control strategies able to ensure a reduction of the vibration level;

The outline of the work is as follows. In Section 2 the whole system is described, with particular emphasis on the semi-active MR devices and on the experimental set-up. In Section 3 the vibrations of the washing machine are measured and analyzed in many different mounting configurations of the passive and MR dampers. In Section 4 the adaptive damping strategies are designed and analyzed. Section 5 ends the work with some conclusive remarks.

2. SYSTEM DESCRIPTION

The washing machine object of this work is a prototype based on the *Ariston Aqualtis* laundry manufactured by *Indesit Company*. It is characterized by a suspended tub which is linked to the machine cabinet thanks to a suspension system. In Fig.2 a simple scheme of the machine is depicted. Note that:

- the suspended mass is linked to the top and chassis panels by two coil springs; it is also linked to the base and chassis panel by two dampers;
- the suspended mass is constituted by the drum, the motor, the fly-wheel, and by the clothes and water in the tub. The rotary drum movements may be clockwise and counter-clockwise, and the maximum spin level is 1400 round-per-minute.

Throughout this work, the *x*-axis, the *y*-axis and the *z*-axis indicate the horizontal, lateral, and vertical direction respectively; the convention used for the “DX” and “SX” sides of the machine is displayed in Fig.2.

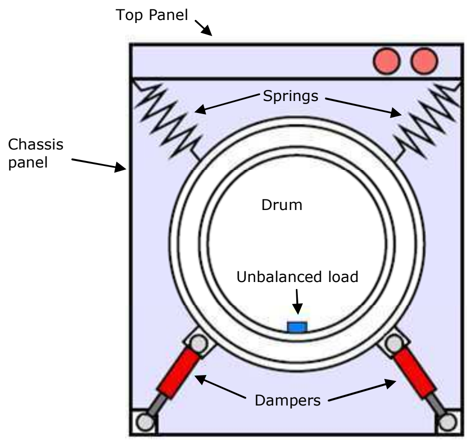

Fig.2. Washing Machine scheme (left) and system reference (right)

As already remarked, the focus in this work is on the role played by the dampers on the vibration and acoustic performance of the machine. The *Aqualtis* laundry is equipped with two standard "passive" (non electronically controlled) dampers, each providing a nominal friction force of 100N. A sample of these dampers is displayed in Fig.3.

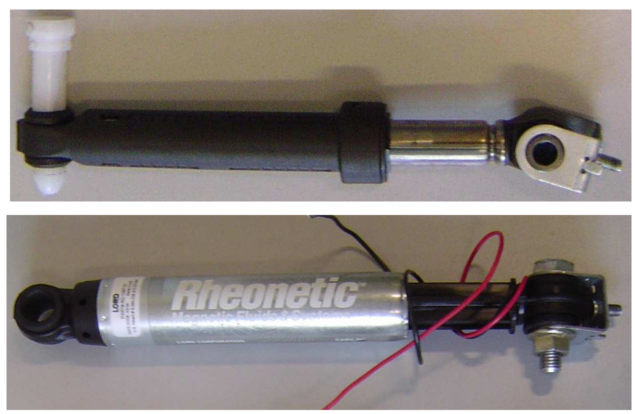

Fig.3. Up: the standard damper of the *Ariston Aqualtis*; down: the controllable *RD-1097-01* friction damper by *Lord* .

The standard damper has been replaced with a sophisticated electronically-controlled device. This is the MR Controllable Friction Damper *RD-1097-01* developed and distributed by *Lord*. This component can change continuously the damping force and it is specifically designed for this kind of applications. The main feature of this device is that the damping force is obtained as friction between foam covering the piston and the external case of the component (this damper is also nicknamed "sponge" damper). This foam is saturated with magnetorheological fluid. By applying a magnetic field to the foam it is possible to change its amount of friction force. The magnetic field is generated by a current in a coil built in the damper piston. The main nominal characteristics of the device are the following:

- maximum and minimum length: 253mm (fully extended) and 195mm (fully compressed) respectively; the body diameter is 32mm;
- the delivered force does not depend on the stroke velocity but on the current command only (whereas an ideal hydraulic damper delivers a force proportional to the stroke velocity - see e.g. [32, 39]); this makes this device a "friction actuator", which is typical of low cost dampers dedicated to washing machine applications;

- the controllable current range is 0A-0.45A (current peaks up to 0.6A are tolerated for a short time during transients); the corresponding force range is 10N-75N (with transient peaks of 110N); see Fig.4 for the complete current-force map. Note that the controllability range is very large, since the ratio between minimum and maximum force is about 1:10. As is well known (see e.g. [34-36]) this high controllability ratio is a very important and appealing feature for semi-active control design purposes.

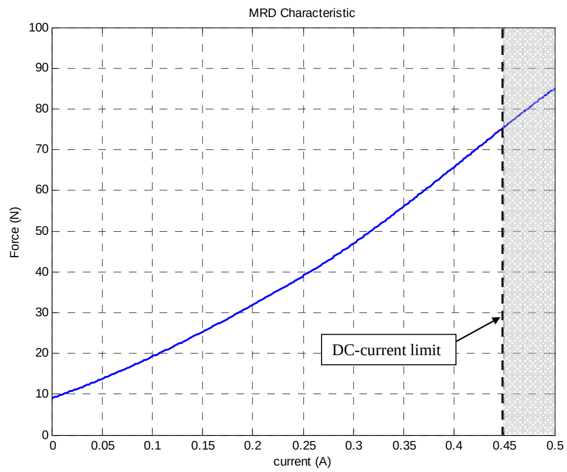

Fig.4. Characteristic of the MR Sponge damper.

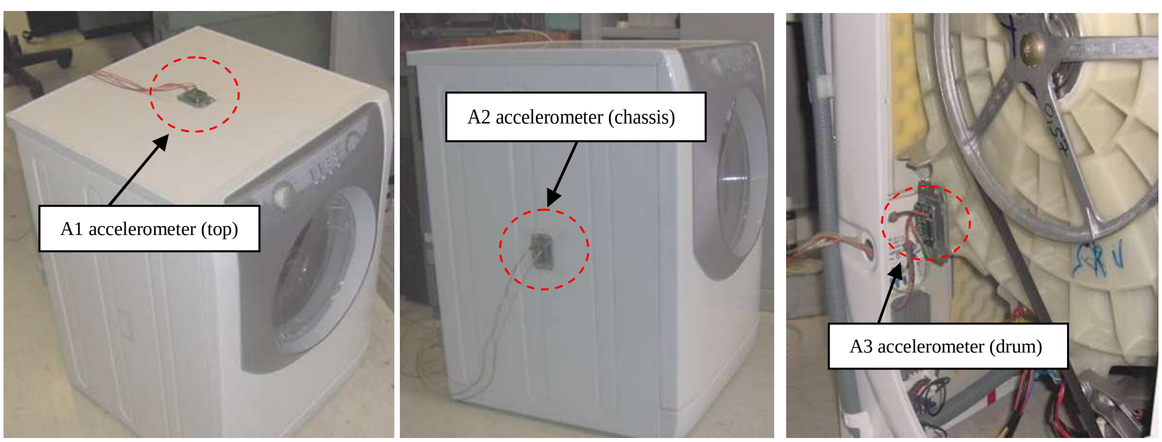

Fig. 5. Sensor positioning. Top panel (A1), chassis panel (A2), and drum (A3) accelerometers.

In order to measure and control the machine vibrations, the washing machine has been equipped with a basic set of sensors, constituted by (Fig.5):

- two 3-axis MEMS accelerometers glued on the top panel (labeled as A1) and on the chassis lateral panel (labeled as A2), characterized by a ±2g range and a bandwidth of 130Hz;
- a 3-axis MEMS accelerometer linked to the drum (labeled as A3), and characterized by a ±6g range and a bandwidth of 130Hz.

These sensors are consistent with the measured acceleration level and the frequency domain of the system dynamics we consider. The acceleration signals are measured with a 16bit ADC module (9215) of the National Instruments cRIO rapid prototyping control unit, at the sampling frequency of 1KHz (Fig.6).

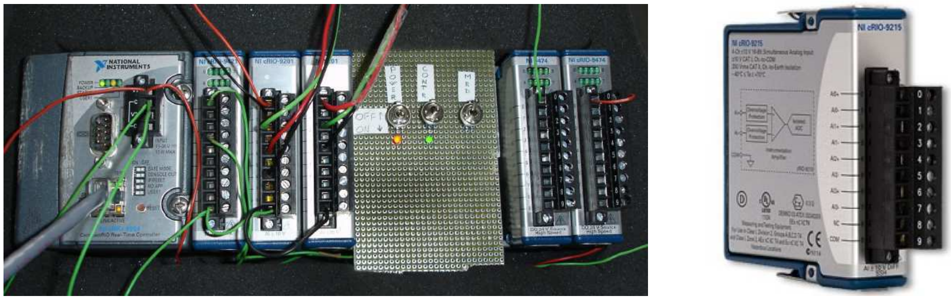

Fig.6. Left: NI cRIO control and acquisition system; right: the 9215 module used for data acquisition.

Under the assumption of a perfectly balanced suspended mass and symmetry, during a spin cycle the drum has rotary movements only ([25]). In case of unbalanced load, some lateral and vertical movements of the suspended mass are induced and transmitted to the cabinet panels through the springs and dampers. The unbalanced load hence is the main cause of vibrations, and the amount of energy transmitted is strictly related (in a direct proportional way) to the rotational speed of the drum.

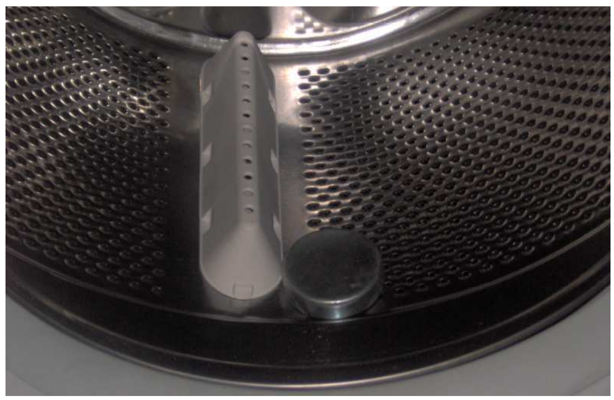

Fig.7. Magnet placed inside the drum, to emulate an unbalanced load.

In order to explore the whole working range of the machine, the following simple experimental protocol has been defined:

- the machine is tested for different spin velocities, from 100rpm to 1400rpm, with 100rpm steps; each spin cycle is 60s-long and it is done at constant speed;
- every set of spin cycles is done for several unbalanced weights. The tested unbalanced weights are 300g, 400g and 500g; for the sake of conciseness, in the rest of the work only the results obtained with the 500g load (the most severe condition) are presented; this load is consistent with an intensive use of the laundry and it is obtained with magnets positioned into the drum (Fig.7).

3. VIBRATION MEASUREMENTS AND CHARACTERIZATION OF THE SYSTEM

The aim of this section is to analyze the behavior of the machine in different configurations: the standard configuration, the “no-dampers” configuration, and some MR-based configurations.

In order to understand the main features of the vibrations which affect the external panels of the laundry at high-speed spin, in Fig.8 the a_{drum} and a_{top} accelerations (measured on the drum and on the cabinet top, as described in Fig.5) are displayed in the time-domain and in the frequency-domain.

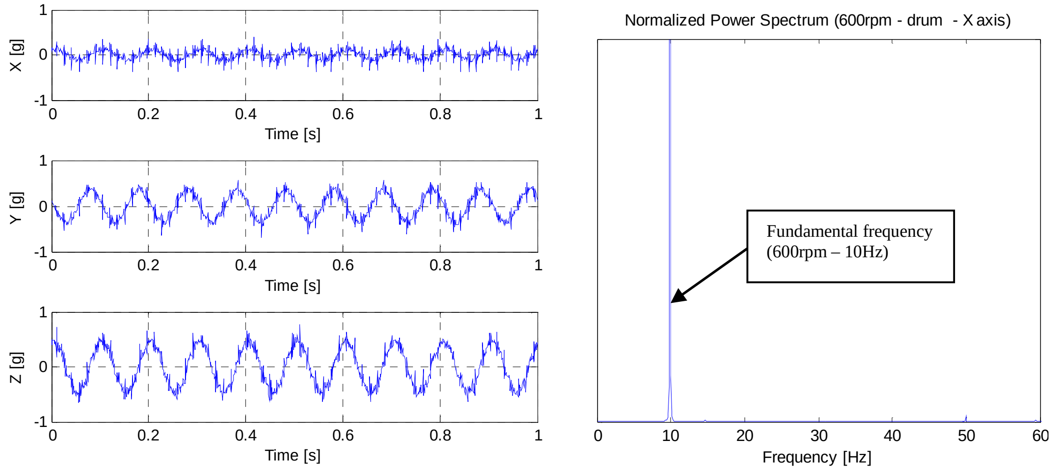

Fig.8a. Left: time-domain behavior of the 3-axis accelerations on the drum at 600rpm. Right: power spectrum of the X-axis.

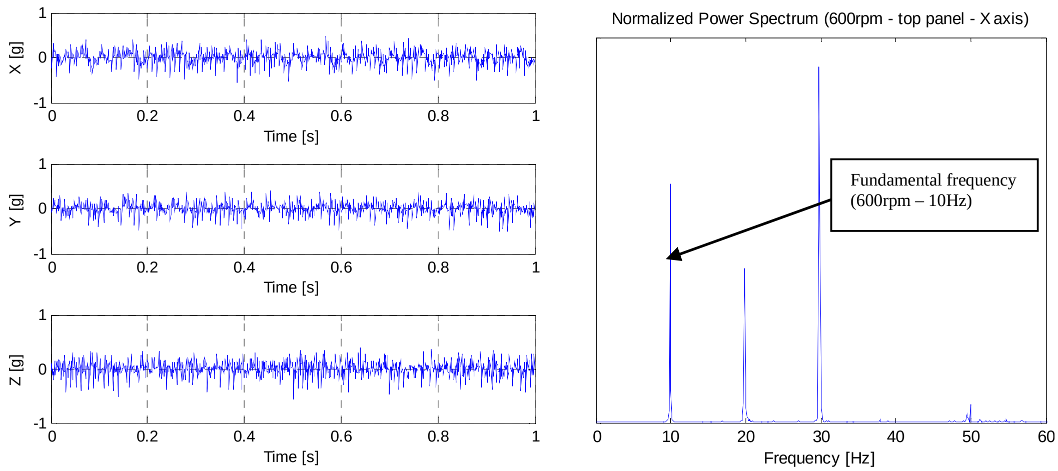

Fig.8b. Left: time-domain behavior of the 3-axis accelerations on the top panel at 600rpm. Right: power spectrum of the X-axis.

From Fig.8 it is clear that the drum is subject to an oscillation which is an almost-pure three-dimensional sinusoid at the fundamental rotation frequency, whereas the spectral content of the panel vibration is much richer since it contains higher harmonics. Moreover, notice that the drum and panel vibrations occur along all the 3 axis of the machine. Regarding the spatial movement of the drum during the spin, it is interesting to analyze the movement of the geometric center of the drum, at different spin speeds. Fig.9 shows its trajectory in the X-Z plane, reconstructed from accelerometer measurements. Notice that at low speed (200rpm) the movement is an ellipse with a dominant vertical axis; by increasing the spin speed, the direction of the movement tends to rotate towards the X-axis and the elliptical trajectory tends to collapse into a 1-dimensional line; this occurs at 600rpm; by further increasing the speed, the trajectory becomes an ellipse again, but the dominant axis is the horizontal. Interestingly enough, the sense of rotation of the drum center changes when crossing the 600rpm speed.

The measurements displayed in Fig.8 and Fig.9 show that the complete characterization of the vibration behavior of the machine is a complex task, since the drum has a complex movement, and the propagation dynamics of the vibration from the drum to the external cabinet are non trivial and non-linear; in this work hence we have adopted a simplified approach (which is consistent with our control-oriented perspective), where the machine vibration is condensed into three vibration indices:

$$J_{top}(\omega) = \sum_{A=x,y,z} \left[\frac{\sum_{t=1}^{N} a_{top}^2(t;A)}{N} \right], \quad J_{chassis}(\omega) = \sum_{A=x,y,z} \left[\frac{\sum_{t=1}^{N} a_{chassis}^2(t;A)}{N} \right], \quad J_{drum}(\omega) = \sum_{A=x,y,z} \left[\frac{\sum_{t=1}^{N} a_{drum}^2(t;A)}{N} \right]. \tag{1}$$

In (1) $a_{top}(t;A)$ is the 3-Axis (A=x,y,z) acceleration signal measured by the top accelerometer (A1); similarly, $a_{chassis}(t;A)$ and $a_{drum}(t;A)$ are the chassis (A2) and drum (A3) accelerations, respectively. It is assumed that the indices (1) are computed from an experiment N-samples long (in case of a 60s experiment with 1KHz sampling frequency, N=60000), with the spin speed kept constant at the value ω. Notice that $J_{top}(\omega)$, $J_{chassis}(\omega)$, $J_{drum}(\omega)$ simply represent the estimated vibration energy measured by the three sensors during a constant-spin cycle ([28, 31]).

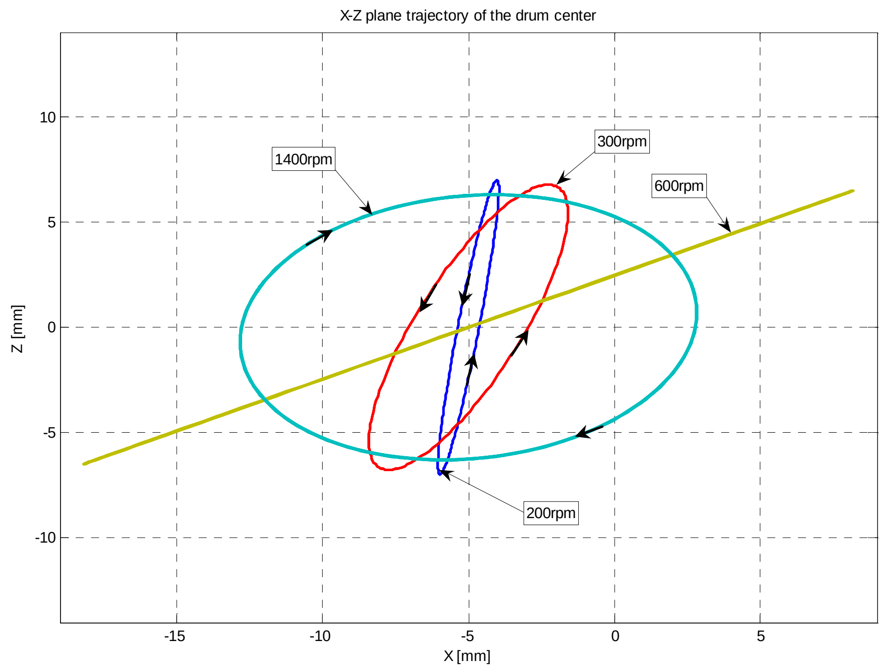

Fig.9. Movement of the drum center, in the x-z plane, at different rotation speeds. The arrows indicate the sense of rotation of the trajectory.

The three indices measured on the machine equipped with the standard passive dampers are illustrated in Fig.10 (the indices are normalized for confidentiality reasons). Some comments can be drawn:

- The drum movements increase with respect to the spin velocity. Indeed the centrifuge force acting on the suspended mass is proportional to the squared spin velocity (ω^2) and to the unbalanced load (m). This quadratic dependence on the spin speed is clear from behavior of the drum index $J_{drum}(\omega)$.
- The drum dynamics show a low-frequency resonance. This is a well known structural resonance and it is due to the elasticity of the spring and the suspended mass. It can vary with respect to the total weight (tub, water, etc.) from 200rpm to 300rpm. In case of the testing condition (unbalanced weight of 500g) the resonance appears at about 250Hz.
- The vibration registered on the top panel and on the chassis panel is significantly smaller than the vibration measured on the drum. This is obvious, since the role of the suspension is to filter the propagation of the source (drum) vibration at the target (top, chassis) position.
- The top panel and the chassis panel show a resonant behavior at 1200rpm and 1400rpm, respectively. Notice that in

correspondence to the resonances, the attenuation ratio of the suspension (ratio between the vibration of the cabinet and the vibration of the drum) is comparatively small.

- From an acoustic point of view, the 1200rpm vibration and the 1400rpm vibration are the most annoying since they have the highest vibration energy; at these resonances the acoustic noise can be clearly perceived.

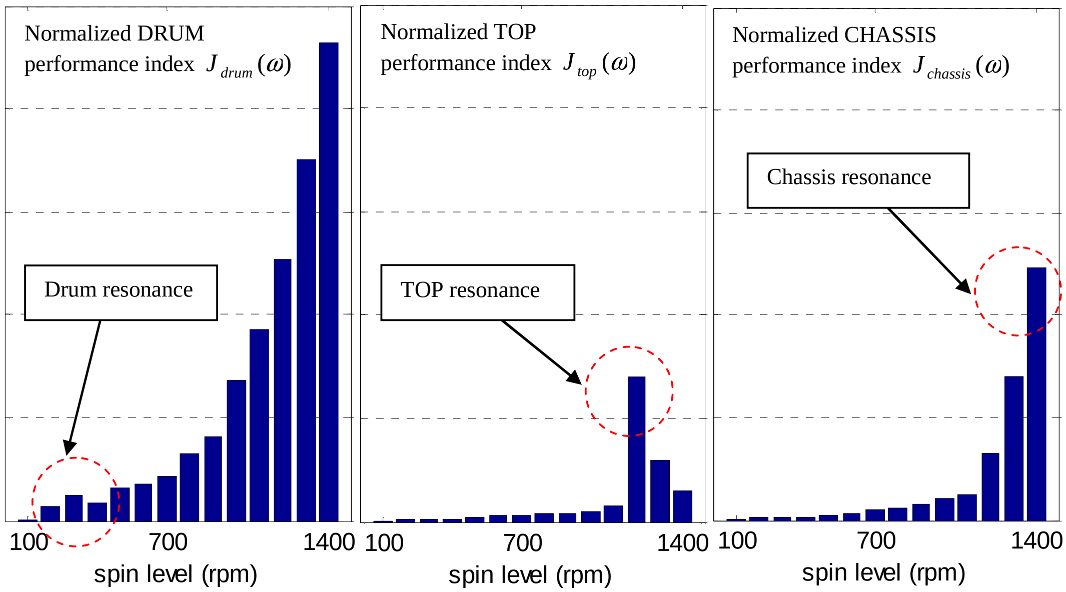

Fig.10. J_{drum} (left), J_{top} (center) and $J_{chassis}$ (right) for different values of spin velocity.

The three indices (1) can be further condensed into a single performance index, say $J_{vib}(\omega)$, which represents the total amount of energy transmitted to the chassis and top panels; it is strictly related to the perceived acoustic noise due to frame vibration of the body cabinet. It is simply the sum of $J_{top}(\omega)$ and $J_{chassis}(\omega)$, namely:

$$J_{vib}(\omega) = J_{top}(\omega) + J_{chassis}(\omega) = \sum_{A=x,y,z} \left[\frac{\sum_{t=1}^{N} a_{top}^2(t;A)}{N} \right] + \sum_{A=x,y,z} \left[\frac{\sum_{t=1}^{N} a_{chassis}^2(t;A)}{N} \right]. \tag{2}$$

Using the condensed vibration index (2), the performance of five different damper configurations have been explored:

- standard configuration: two passive dampers;
- dampers completely removed (NO dampers);
- two MR dampers, driven by the fixed current which provides the minimum vibration level
- one MR dampers only, mounted on the left-side position (SX position in Fig.2), driven by the fixed current which provides the minimum vibration level; right-side damper removed;
- one MR dampers only, mounted on the right-side position (DX position in Fig.2), driven by the fixed current which provides the minimum vibration level; left-side damper removed.

The best fixed-current level for each MRD configuration has been achieved by direct search of the current in the range 0A-0.45A which minimizes $J_{vib}(\omega)$. This optimization procedure is omitted for the sake of conciseness. It is interesting to notice, however, that every configuration and every spin velocity has its own "best" current; the best current usually is not in a trivial position (0A or 0.45A).

The entire analysis is summarized in Fig.10, where the performance index (2) is plotted as a function of the spin velocity ω, for all the configurations. The results are insightful, and some interesting considerations can be drawn.

- The vibration phenomena are well visible in the spin velocity range 1100rpm-1400rpm. As a matter of fact the drum energy increases with respect to the square of spin rate, but only from 1100rpm it is strongly transferred to the panels. Therefore, for the rest of the work the vibration analysis will focus mainly on the high-velocity range.

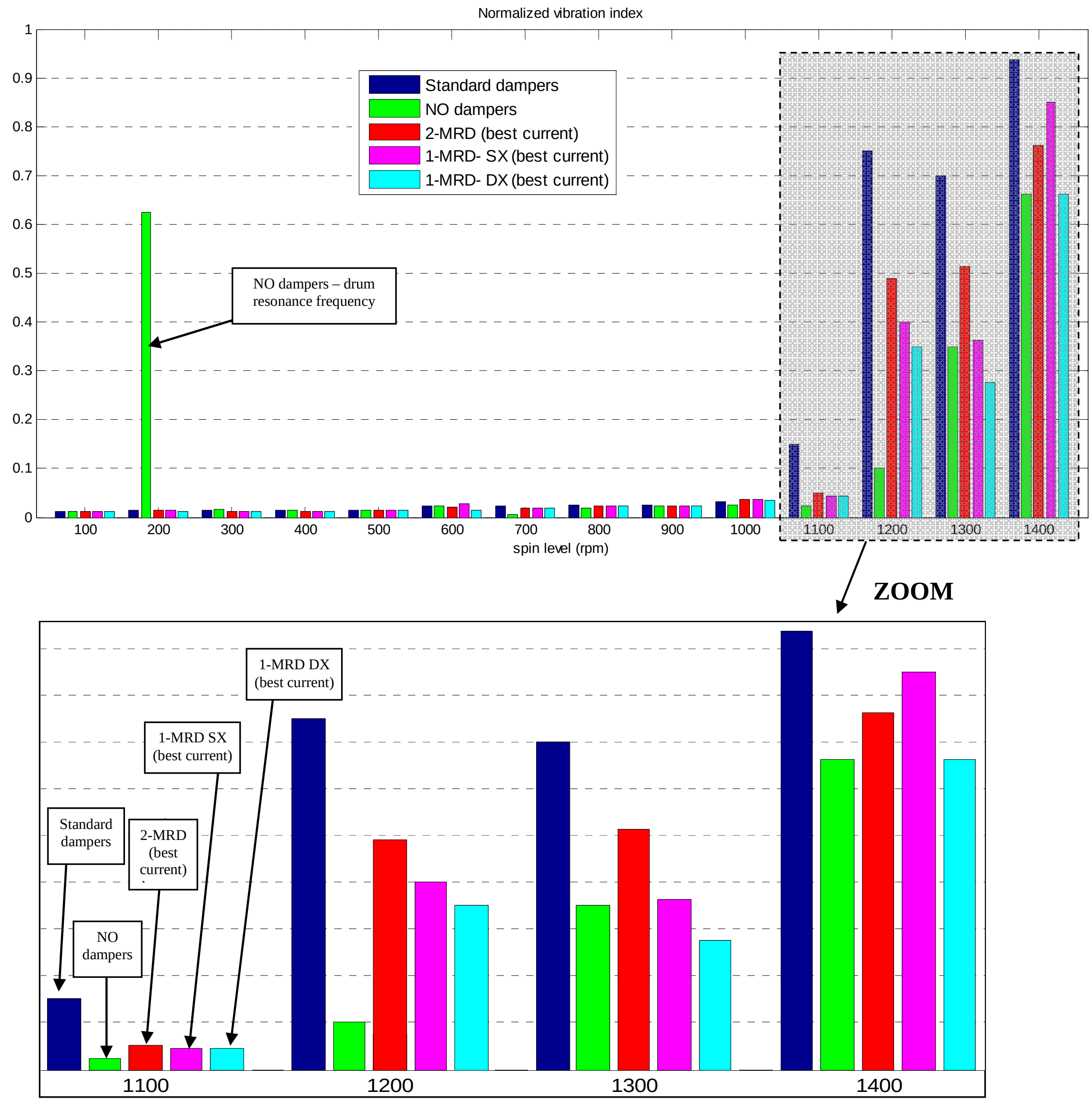

Fig.10. Performance index $J_{vib}(\omega)$ for different dampers mounting configurations.

- In case of no dampers, the drum dynamics are transferred to the frame through the coil springs only. It is interesting to observe that this configuration provides – almost everywhere – the best attenuation results. However this configuration cannot be used since the 200rpm resonance is not damped. This causes large movements of the suspended mass which hits the top panel, with consequent vibration and damages to the entire structure. This problem is clearly visible in Fig.10 by the energy "spike" at 200rpm for the NO-dampers configuration.
- The configurations with MR dampers always outperform the configuration with passive dampers. This occurs for every value of spin, including the drum-resonance frequency.
- The single MR damper configuration outperforms the configuration with two MR dampers. Interesting enough, the resonance at 200rpm is well damped also with a single damper.
- The performances obtained with a single MR damper are not symmetric: the right-side (DX) location uniformly

guarantees best performance everywhere. This can be easily explained by the non symmetric features of the machine. The results of the analysis condensed in Fig.10 clearly show that the filtering performance of the standard dampers can be significantly improved by means of MR-dampers. An interesting outcome of the analysis is that the 2-passive-dampers configuration can be successfully replaced by a single-MR-damper configuration, where the damper is placed on the “DX” side of the machine.

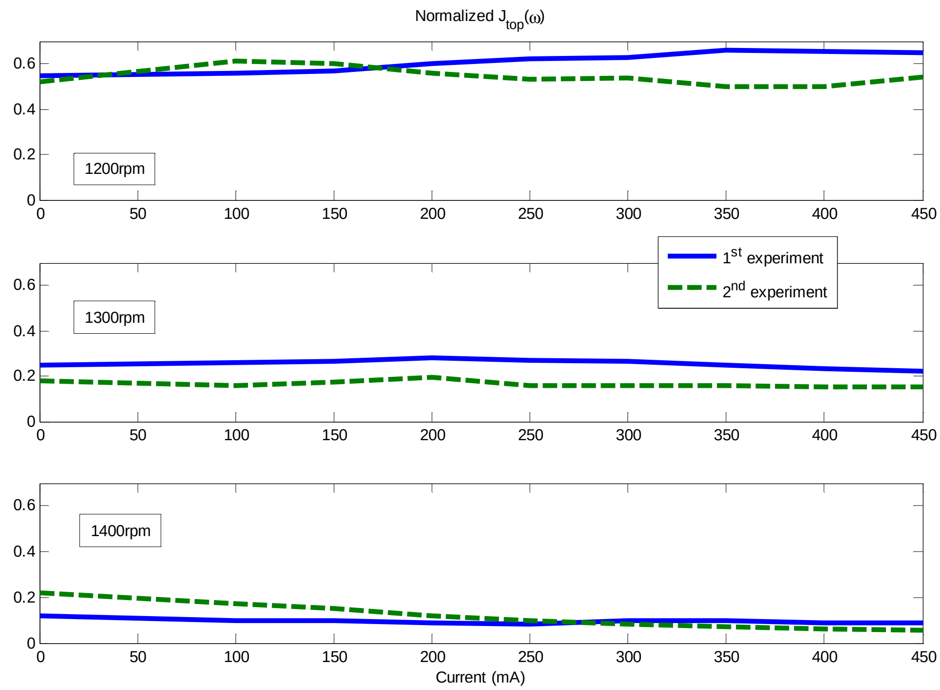

Fig.11. Performance index $J_{top}(\omega)$ for the MR damper at the “DX” side, for different values of current. Two repeated experiments.

The analysis above outlined seems to suggest a simple way of optimizing the filtering performance of the laundry suspension: use a 1-MRD-DX configuration and schedule the MRD current as a function of the spin velocity ω. This solution is very simple since the control logic is a pure open-loop look-up table of the MRD current as a function of ω. However, two major question arise:

1. Is the optimal current-speed mapping robust with respect to system variations (such as load and water weight in the tub, damper wearing, temperature, unbalanced load, etc…), or a run-time adaptation strategy must be designed?
2. Is the fixed-current strategy (with our without a run-time adaptation) the best way of using the electronically-controlled MR-damper, or a better vibration filtering can be obtained by a more sophisticated modulation strategy of the MRD current?

The first issue has a simple answer, which can be easily illustrated by inspecting the experimental results displayed in Fig.11, where the performance index $J_{top}(\omega)$ is displayed as a function of the MRD current, for the three most interesting spin speeds: 1200rpm, 1300rpm, 1400rpm. The results of two experiments repeated in the same conditions are reported. The results clearly indicate that low repeatability of $J_{top}(\omega)$. Notice that not only the curves of the two experiments are not overlapped, but the optimal current changes (see e.g. the case of 1200rpm, where the best current is 50mA in the first experiment, 350mA in the second experiment). This dispersion of the experimental results is due to the complex path of propagation of the vibration, the fact that $J_{top}(\omega)$ is constituted by the sum of a large number of harmonics, and the change of features of the MR-damper with respect to temperature and wearing.

Hence we can conclude that, in order to achieve always the best filtering performance, ad adaptive method for on-line estimation of the best MRD-current is required. This will be the topic of the next section.

4. ADAPTIVE-DAMPING CONTROL STRATEGIES

In this section the adaptive control of the MR damper located on the DX side of the laundry is discussed. As already pointed out at the end of the previous section, the first control objective is to find the best current (fixed) value in a constant-spin working condition. It has been shown that the best current value can significantly vary in different repeated experiments; a run-time optimization hence is required.

The adaptation technique proposed herein is very simple, but it is consistent with the specific features of this application. It can be summarized as follows:

- when a constant-spin condition starts, the training phase is activate: the algorithm explores the whole current range with a comparatively slow ramp signal, possibly repeated several times;
- during this training phase, the instantaneous vibration level is measured, and a current→vibration map is built;
- at the end of the training phase, the current value corresponding to the minimum vibration level is computed, using a smoothed version of the current→vibration map; this "optimal" current is then applied for the remaining phase of the constant-spin condition.

The vibration index used in the above procedure is the same used in (2), with the slight difference of being an "instantaneous" index (not averaged over N samples, i.e. N=1), namely:

$$J_{vib}(\omega,t,I_{MRD}) = \sum_{A=x,y,z} a_{top}^2(t;A,I_{MRD}) + \sum_{A=x,y,z} a_{chassis}^2(t;A,I_{MRD}) \,. \qquad (3)$$

With a slight abuse of notation we use the same name J_{vib} both for (2) and (3). Notice that in the optimization procedure described above the instantaneous index (3) is required, since the system is forced to be time-varying. Also notice that in (3) the dependence of J_{vib} on the MRD current I_{MRD} is emphasized.

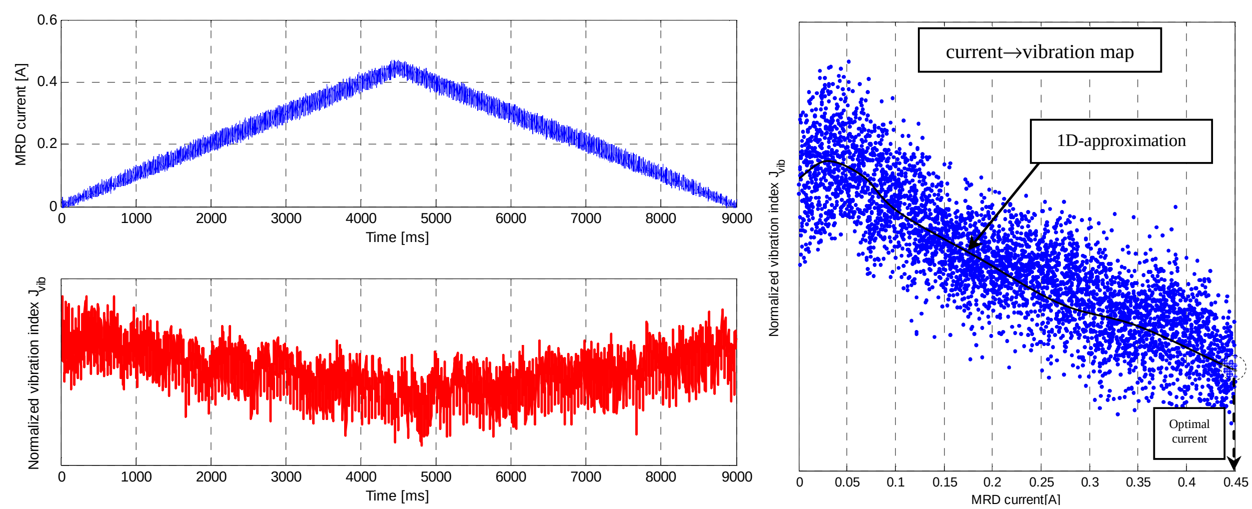

Fig.12. Example of optimization cycle (1400rpm). Left/top: slowly-varied MRD current; left/bottom: istantaneous vibration index; right: current-vibration map, and its 1D-approximation.

The literature of adaptive control is vast, and a lot of methods and techniques have been proposed (see e.g. [5, 15-17, 23] and references cited therein). The approach described above, however, is not a genuine adaptive-control method; it can be better classified as a batch optimization procedure performed on-line, when required. The choice of this simple approach is motivated by some peculiar features of this application:

- the controlled signal is not a single one, but a non-trivial combination of six acceleration signals;
- the relationship between the MRD current and the vibration index is non linear and not monotonically increasing/decreasing (see Fig.11);
- the system is very noisy and the optimization/adaptation procedure must be terminated in a short time (only a few seconds are allowed to complete this optimization routine).

An example of the current-optimization cycle is illustrated in Fig.12, for the 1400rpm condition. Note that the current range 0A-0.45A is explored with a double ramp, in 9s. It is clear the dependence of the vibration index on the MRD current. The current-vibration map is also displayed with its averaged (smoothed) counterpart, which shows that the 0.45A current is – for this experiment – the best choice.

An example of the training phase followed by the constant-current condition is illustrated in Fig.13. Note that the training phase has been shortened and lasts only 3s (this is the maximum amount of time which can be accepted for optimization purposes); also notice that the training phase is constituted by six consecutive current ramps. A long/cumbersome analysis (here not reported for the sake of conciseness) has shown that – given an amount of time for the training phase – it is preferable to use many (fast) ramps, instead of a single (slow) current ramp. Note that after the training phase the current is fixed to the optimal value and kept constant till the end of the spin cycle.

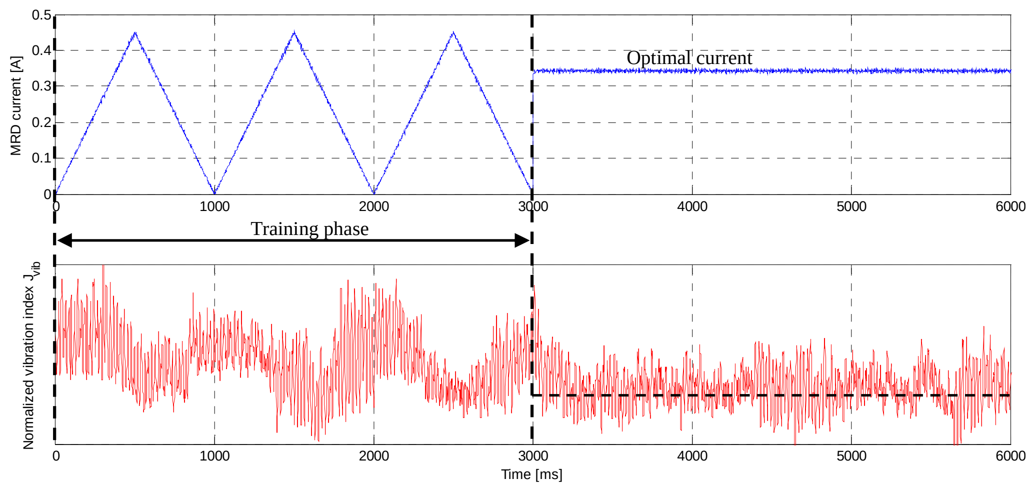

Fig.13. Example of a complete training phase, followed by the optimal-current working condition (1400rpm). Top: MRD current; bottom vibration index.

At the end of the previous section, an issue has been raised: is the above batch-optimized fixed-current strategy the best one, or a better vibration filtering can be obtained by a more sophisticated modulation strategy of the MRD current?

Notice that, in this application, it is hard to resort to standard semi-active feedback control strategies typically used on vehicles (see [2, 6, 8, 13, 18, 21, 26, 29, 40-41]), for many reasons: first, the machine dynamics from the drum to the cabined can hardly be approximated by a 1-dimensional mass-spring-damper model; moreover, no direct measurement of the acceleration at the cabinet-side attachment of the damper is available; finally, it is unclear if the minimization of the vibration at the cabinet-side attachment of the damper is the right control objective.

Even if the semi-active algorithms used on vehicles cannot be directly resorted to, they can suggest a possible way of modulating the MRD current: it has been shown (see e.g. [29, 34-36]) that, beyond the main system resonance, the best filtering performance can be achieved by a sinusoidal modulation of the damping force, at the same frequency of the disturbance; moreover, the best results are typically achieved by using the whole available modulation range. The candidate best control signal hence has the following expression:

$$I_{MRD}(t) = \frac{0.45A}{2}\sin(\omega t + \Phi) + \frac{0.45A}{2}, \tag{4}$$

where ω is the spin angular speed (e.g. $\omega = 2\pi \cdot 20$ rad/s if the spin velocity is 1200rpm), and Φ is the phase-shift of the sinusoidal signal. Notice that in (4) the 0A-0.45A current range is fully used.

A tricky functional optimization problem hence is recast into a simple single-parameter optimization problem, where the parameter to be optimized is Φ.

This approach is concisely described in Fig.14, where the optimization procedure of the phase-shift of the sinusoidal current signal is outlined, for the 1400rpm condition. Notice that the training phase is 20s-long; during this phase Φ is slowly varied in the range 0°-360°, and a map which correlates the phase-shift Φ with the vibration index is built. At the end of this procedure the phase-shift providing the best attenuation is selected and kept constant for the rest of the spin cycle. Notice that this procedure works correctly, and the vibration index is minimized.

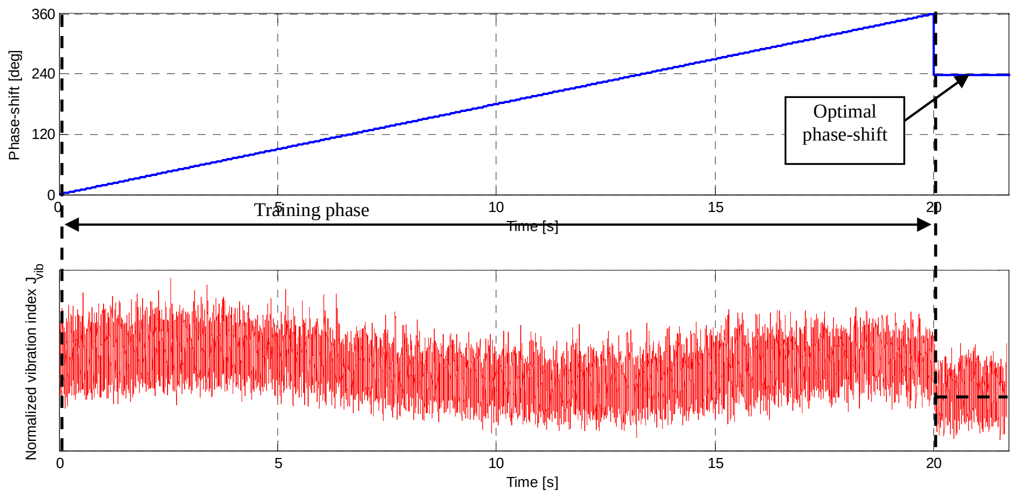

Fig.14. Phase optimization procedure in tome domain. 1200rpm spin.

The two optimization (or parameter-adaptation) procedures presented above can be summarized as follows:

- optimization of the fixed-current;
- optimization of the phase-shift of a sinusoidal current modulated at the frequency of the current spin speed.

The first procedure is the most simple and intuitive; the second has been heuristically designed, by inheriting the typical behavior of a standard semi-active algorithm.

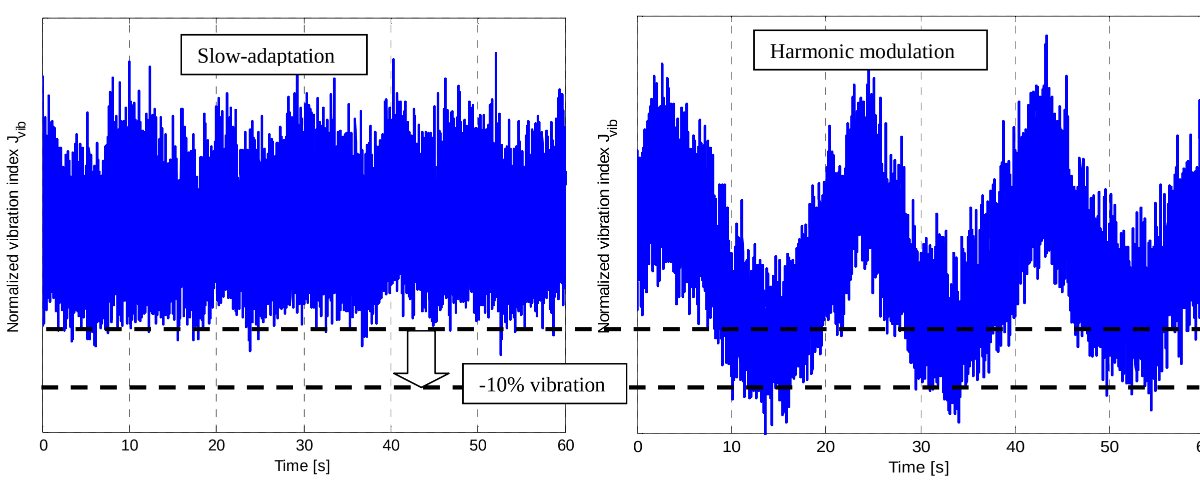

Fig.15. Comparison of the fixed-current variation (left) and the sinusoidal-current phase variation (right), at 1300rpm.

In Fig.15 a comparison of the two adaptation procedures is outlined. The two optimization parameters are varied in their whole range, during 60s-long experiments; In Fig.15 the corresponding behavior of the vibration index is displayed. Notice that in this experiment (run at 1300rpm), changing the simple (fixed) current has a negligible effect on the vibration index. Instead, the sinusoidal modulation of the current at the spin frequency shows the high sensitivity of the vibration index with respect to the phase-shift of the sinusoid. It is interesting to observe that the more sophisticated sinusoidal modulation of the current provides a performance improvement of about 10%.

The above experiment shows that the sinusoidal modulation strategy can further improve the performance provided by a simple optimization of the fixed current. However this more sophisticated control strategy has two main intrinsic problems:

- the first main problem is the duration of the training-phase: it has been shown that the optimization of the fixed current can be reduced to 3s; the optimization of the phase shift can hardly be reduced below 10s (this analysis is not reported here for the sake of conciseness); unfortunately 10s devoted to the training phase are unacceptable;
- the second main problem is the sensitivity of this procedure to the rotation frequency: in order to achieve good vibration-reduction results the current must be modulated exactly at the spin frequency, with a tolerance on the frequency estimation of no more than 0.05%; unfortunately the standard system used in a washing machine for the control of the drum rotation speed has a tolerance of about 1%. A sophisticated algorithm for the run-time estimation of the actual rotation frequency hence must be implemented (see e.g. [3, 30, 33]).

Overall, we can conclude that the simpler optimization strategy of the fixed current probably guarantees the best trade-off between performance and complexity.

5. CONCLUSIONS

In this work the idea of using electronically-controlled dampers for improving the vibration in a washing machine has been developed. The actuator is a low-cost friction magnetorheological damper. The idea is to adapt on-line the damping characteristics in order to reduce vibration level of the machine panels.

The system has been accurately analyzed and different mounting positions of the dampers have been tested. The design and testing procedure of two different adaptive algorithms has been proposed. The control system has been implemented on a rapid prototyping ECU and tested on a washing machine instrumented with three 3-axis MEMS accelerometers.

This work has proven the effectiveness of replacing the standard passive dampers with electronically-controlled ones. Interestingly enough, it has been shown that a single MR device ensures an adequate damping of the drum resonance and a better vibration filtering at high-speed spin. Some test have highlighted the effectiveness of the proposed control strategies.

REFERENCES

[1] Atray V.S., P.N. Roschke (2003). Design, fabrication, testing, and fuzzy modeling of a large magnetorheological damper for vibration control in a railcar. IEEE/ASME Joint Rail Conference, pp.223-229.

[2] Ahmadian M., B.A. Reichert, X. Song (2001). System Nonlinearities Induced by Skyhook Dampers. Shock and Vibration, vol.8, n.2, pp.95-104.

[3] Bittanti S., Savaresi S.M. (2000). On the parametrization and design of an Extended Kalman Filter Frequency Tracker. IEEE Transactions on Automatic Control, vol.45, n.9, pp.1718-1724.

[4] Campi M.C., Lecchini A., Savaresi S.M. (2003). An application of the Virtual Reference Feedback Tuning (VRFT) method to a benchmark active suspension system. European Journal of Control, Vol.9, pp.66-76.

[5] Campi M., S.M. Savaresi (2006). Direct nonlinear control design: the Virtual Reference Feedback Tuning (VRFT) approach. IEEE Transactions on Automatic Control, Vol.51, n.1, pp.14-27.

[6] Caponetto R., O. Diamante, G. Fargione, A. Risitano, D. Tringali (2003). A soft computing approach to Fuzzy Sky-Hook control of semi-active suspension. IEEE Transactions on Control System Technology, vol.11, n.6, pp.786-798.

[7] Chrzan M.J., J. David Carlson (2001) MR Fluid Sponge Devices and Their Use in Vibration Control of Washing Machines. Proceedings of the 8th Annual Symposium on Smart Structures and Materials. Newport Beach, CA, USA.

[8] Choi S.B., H.K. Lee, E.G. Chang (2001). Field test results of a semi-active ER suspension system associated with skyhook controller. Mechatronics, vol.11, n.3, pp.345-353.

[9] Fialho I., Balas G.J. (2002). Road adaptive active suspension design using linear parameter-varying gain-scheduling. IEEE Transactions on Control Systems Technology, vol.10, pp.43-54.

[10] Fischer D., R. Isermann (2003). Mechatronic semi-active and active vehicle suspensions. Control Engineering Practice, vol.12, n.11, pp.1353-1367.
[11] Fu-Cheng W., Smith M.C. (2002). Controller parameterization for disturbance response decoupling: application to vehicle active suspension control. IEEE Transactions on Control Systems Technology, vol.10, n.3, pp.393-407.
[12] Fujimori K., Hayakawa K., Kimura H., Matsumoto K., Suzuki Y., Yamashita M. (1999). Robust H∞ output feedback control of decoupled automobile active suspension systems. IEEE Transactions on Automatic Control, vol.44, n.2, pp.392 -396.
[13] Giuia A., C. Seatzu, G. Usai (1999). Semiactive suspension design with an optimal gain switching target. Vehicle System Dynamics, Vol. 31, No. 4, pp. 213-232.
[14] Goodall R.M., W. Kortüm (2002). Mechatronic developments for railway vehicles of the future. Control Engineering Practice, Vol.10, pp.887-898.
[15] Goodwin G. C., K. S. Sin (1984). Adaptive Filtering Prediction and Control. Englewood Cliffs, NJ: Prentice-Hall.
[16] Guardabassi G.O., S.M. Savaresi (2001). Approximate Linearization via Feedback - an Overview. Survey paper on Automatica, Vol.27, pp.1-15.
[17] Hjalmarsson H., M. Gevers, S. Gunnarson, O. Lequin (1998). Iterative feedback tuning: Theory and applications. IEEE Control System Magazine, vol.18, n.4, pp.26–41.
[18] Hong K.S., H.C. Sohn, J.K. Hedrick (2003). Modified Skyhook Control of Semi-Active Suspensions: A New Model, Gain Scheduling, and Hardware-in-the-Loop Tuning. ASME Journal of Dynamic Systems, Measurement, and Control, Vol.124, n.1, pp.158-167.
[19] Hrovat, D. (1997). Survey of Advanced Suspension Developments and Related Optimal Control Applications. Automatica, Vol.33, n.10, pp. 1781-1817.
[20] Isermann R. (2003). Mechatronic Systems: Fundamentals. Springer Verlag, UK.
[21] Kawabe T., O. Isobe., Y. Watanabe, S. Hanba, Y. Miyasato (1998). New semi-active suspension controller design using quasi-linearization and frequency shaping. Control Engineering Practice, Vol.6, n.10, pp. 1183-1191.
[22] Kitching K.J., D. J. Cole, D. Cebon (2000). Performance of a Semi-Active Damper for Heavy Vehicles. ASME Journal of Dynamic Systems, Measurement, and Control, Vol.122, n.3, pp.498-506.
[23] Landau I.D. (1979). Adaptive Control—The Model Reference Approach. New York: Marcel Dekker.
[24] Lord Corporation (2001). Adaptive Off-State Control Method. US Patent 6.311.110.
[25] McDonald K.T. (1998) Physics in the Laundromat. American Journal of Physics. Volume 66, Issue 3, pp. 209-211.
[26] Nakai H., S. Oosaku, Y. Motozono (2000). Application of Practical Observer to Semi-Active Suspensions. ASME Journal of Dynamic Systems, Measurement, and Control, Vol.122, n.2, pp.284-289.
[27] Papadopoulos E., I. Papadimitriou (2001): Modeling, Design and Control of a Portable Washing Machine during the Spinning Cycle Proceedings of the 2001 IEEE/ASME International Conference on Advanced Intelligent Mechatronics Systems
[28] Pintelon R., Schoukens J. (2001). System Identification: a Frequency Domain Approach. IEEE Press, New York.
[29] Rajamani R., S. Larparisudthi (2004). On invariant points and their influence on active vibration isolation. Mechatronics, vol.14, n.2, pp.175-198.
[30] Savaresi S.M. (1997). Funnel Filters: a new class of filters for frequency estimation of harmonic signals. Automatica, vol.33, n.9, pp.1711-1718.
[31] Savaresi S.M., R. Bitmead, W. Dunstan (2001). Nonlinear system identification using closed-loop data with no external excitation: the case of a lean combustion process. International Journal of Control, vol.74, pp.1796-1806.
[32] Savaresi S.M., S. Bittanti, M. Montiglio (2005). Identification of semi-physical and black-box non-linear models: the case of MR-dampers for vehicles control. Automatica, vol.41, pp.113-117.
[33] Savaresi S.M., S. Bittanti, H.C. So (2003). Closed-form Unbiased Frequency Estimation of a Noisy Sinusoid Using Notch Filters. IEEE Transactions on Automatic Control, Vol.48, n.7, pp.1285-1292.
[34] Savaresi S.M., E. Silani, S. Bittanti (2005). Acceleration-driven-damper (ADD): an optimal control algorithm for comfort-oriented semi-active suspensions. ASME Transactions: Journal of Dynamic Systems, Measurement and Control, vol.127, n.2, pp.218-229.
[35] Savaresi S.M., C. Spelta (2007): A Single-Sensor Control Strategy for Semi-Active Suspensions. IEEE Transaction on Control System Technology. (to appear)
[36] Savaresi S.M., C. Spelta (2007). Mixed Sky-Hook and ADD: Approaching the Filtering Limits of a Semi-Active Suspension. ASME Transactions: Journal of Dynamic Systems, Measurement and Control, vol.129, n.4, pp.382-392.
[37] Silani E., Savaresi S.M., Bittanti S., Fischer D., Isermann R. (2004). Managing Information redundancy for the design of fault-tolerant slow-active controlled suspension. Tire Technology International, vol.2004, pp. 128-133.
[38] Silani E., S.M. Savaresi, S. Bittanti, A. Visconti, F. Farachi (2003). The concept of performance-oriented yaw-control systems: vehicle model and analysis. SAE Transactions, Journal of Passenger Cars - Mechanical Systems. vol.2002, ISBN n. 0-7680-1290-2, pp.1808-1818.
[39] Spencer B.F. Jr., S.J. Dyke, M.K. Sain, J.D. Carlson (2003). Phenomenological Model of a Magnetorheological Damper. ASCE Journal of Engineering Mechanics, Vol. 123, No. 3, pp. 230-238.
[40] Tseng H.E., J.K. Hedrick (1994). Semi-active control laws – Optimal and Sub-Optimal. Vehicle System Dynamics, vol.23, pp.545-569
[41] Yao, G.Z., F.F. Yap, G. Chen, W.H. Li, S.H. Yeo (2002). MR damper and its application for semi-active control of vehicle suspension system. Mechatronics, vol.12, n.7, pp.963-973.